

Physical Status of the Intracluster Medium Investigated through Radio and X-ray Observations

Motokazu Takizawa
(Yamagata University)

Itahana, Takizawa et al. (2015), PASJ, 67, 113

Itahana, Takizawa et al. PASJ accepted, arXiv:170807004

Sugawara, Takizawa et al. PASJ accepted, arXiv:1708.09074

DTA workshop 2017

8 November 2017@NAOJ Mizusawa

Radio Halos / Relics

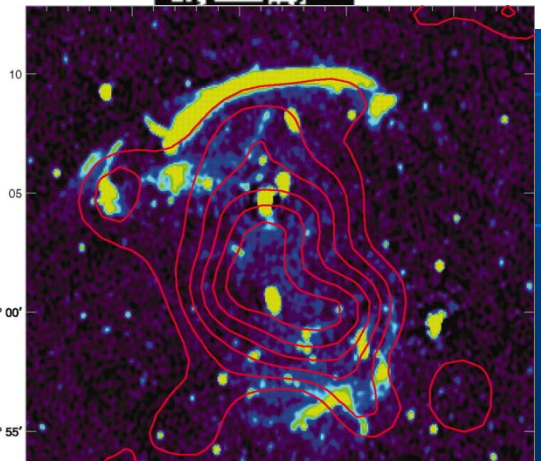
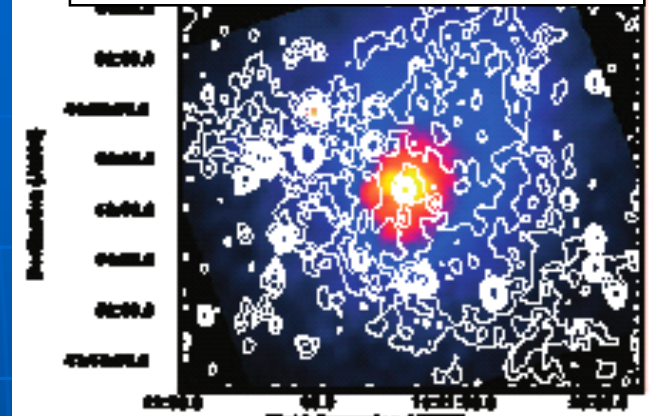
- Some merging clusters have diffuse non-thermal radio emitting regions.
($E_e \sim \text{GeV}$, $B \sim \mu\text{G}$)
- Radio halos and (mini halos)
 - Located near the center, similar to X-ray morphology
 - Associated with ICM turbulence???
- Radio relics
 - Located in the outskirts, arc-like shape,
 - Likely associated with ICM shocks?

Abell 2319 with Radio Halo

Rosat X-ray image (colors)

Radio image (contours)

Feretti et al. 1997



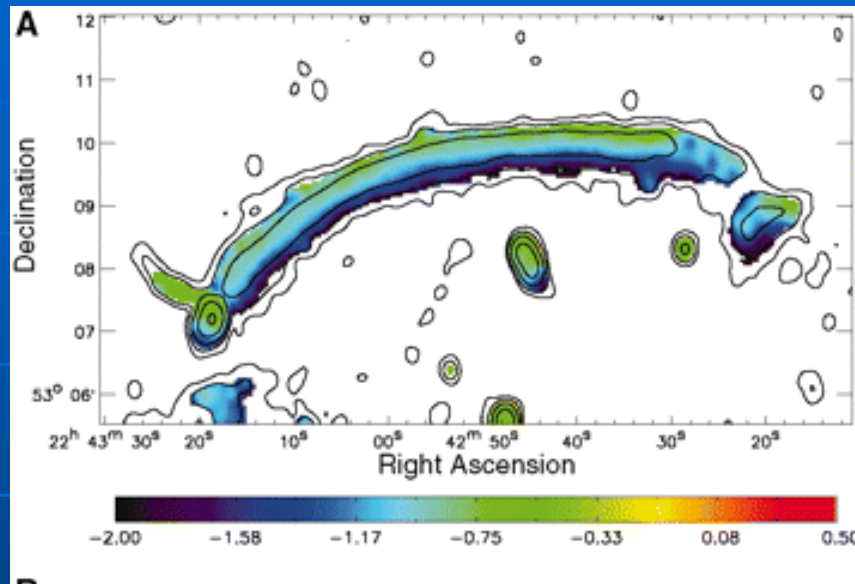
CIZA J2242.8+5301 with Radio Relic

Rosat X-ray image (contours)

Radio image (colors)

Van Weeren et al. 2010

Mach Number Estimation of Shocks at Radio Relics: Two Methods

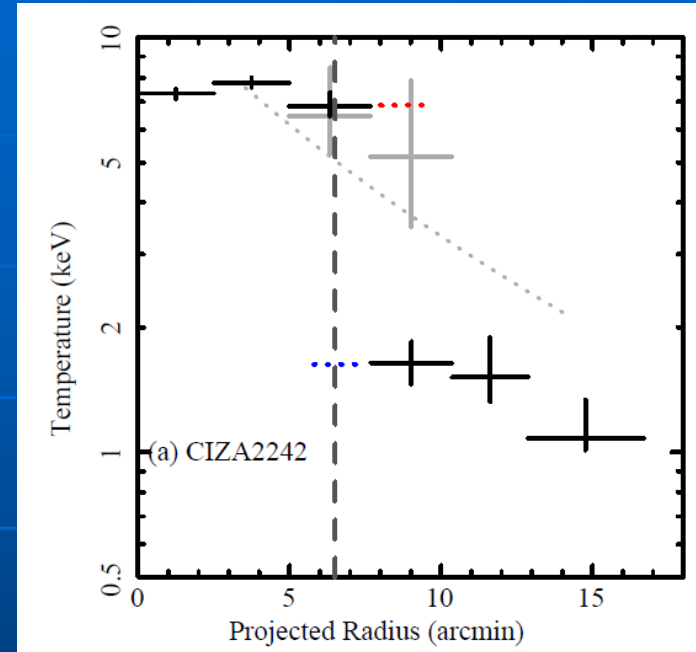


Radio Spectral index map of the relic in CIZA J2242.8+5301 (Van Weeren et al. 2010)

$$F_{\nu} \propto \nu^{-\alpha} \rightarrow N(E_e) \propto E_e^{-(2\alpha+1)}$$

With a (simple) diffusive shock acceleration model,

$$M^2 = (2\alpha + 2) / (2\alpha - 2)$$

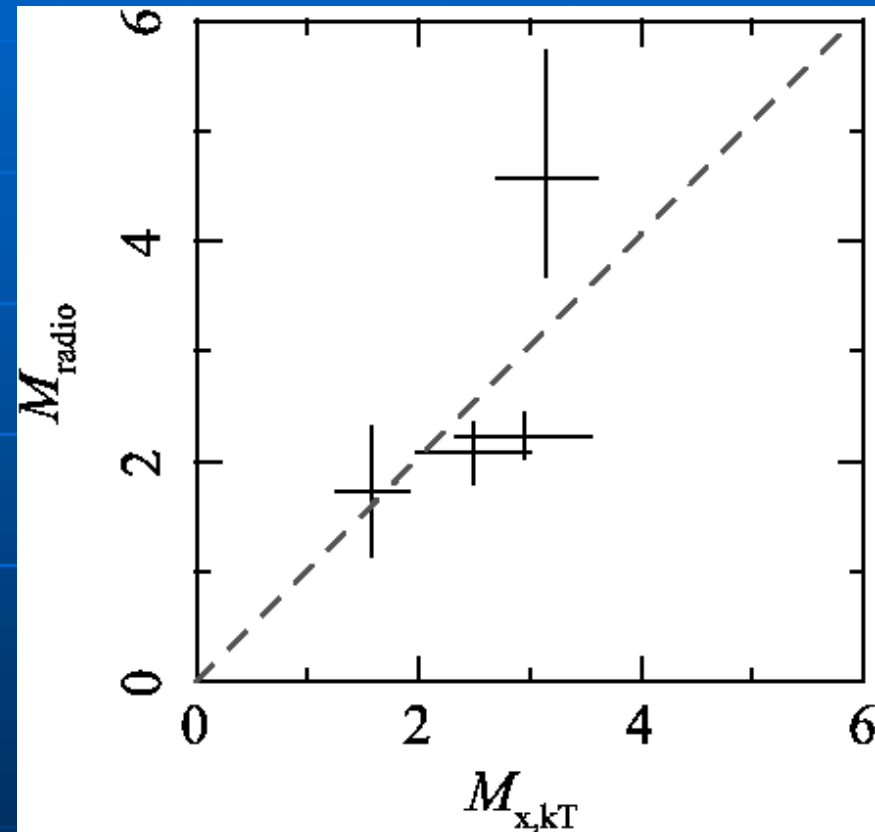


Temperature Profile across the relic in CIZA J2242.8+5301 (Akamatsu & Kawahara 2013)
With the RH relation

$$T_{\text{post}}/T_{\text{pre}} = (5M^4 + 14M^2 - 3) / (16M^2)$$

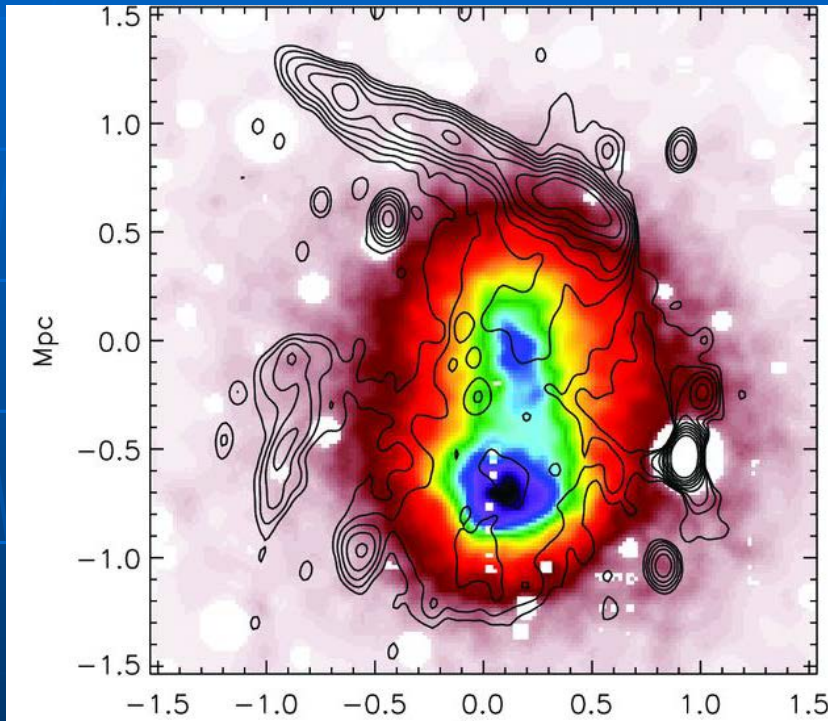
Radio Relics: Mach Number consistency???

- Akamatsu&Kawahara (2013) suggests that M_x and M_{radio} seem to be consistent with each other.
- A simple model of diffusive shock acceleration is correct?
- However, sample size is obviously too small to say something definite.



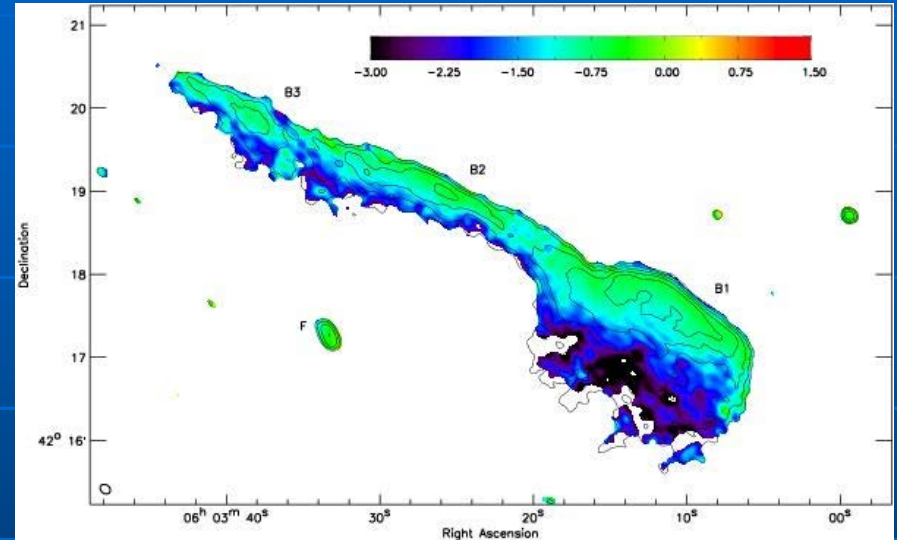
Akamatsu&Kawahara (2013)

1RXS J0603.3+4214 with “toothbrush-relic”



Ogreaan et al. (2013)

Colors: X-ray(XMM)
Contours: radio(WSRT)



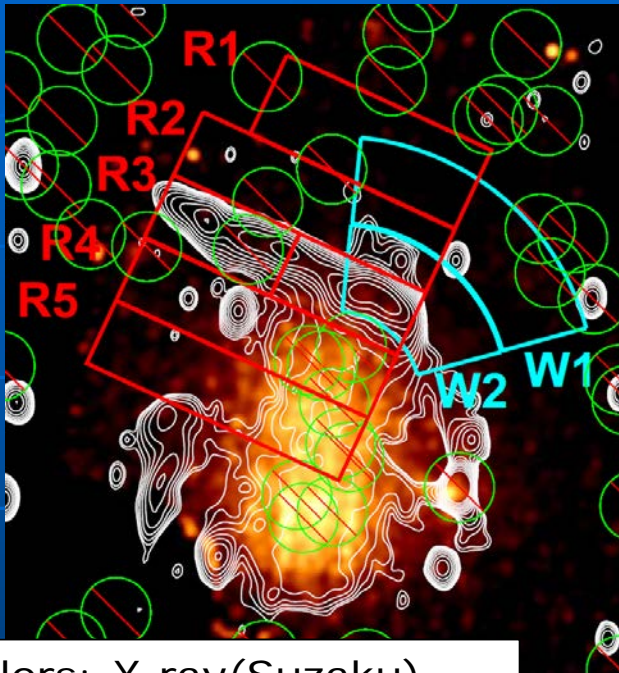
Radio spectral index map
(van Weeren et al. 2012)

$$\alpha_{inj} = 0.6 - 0.7$$

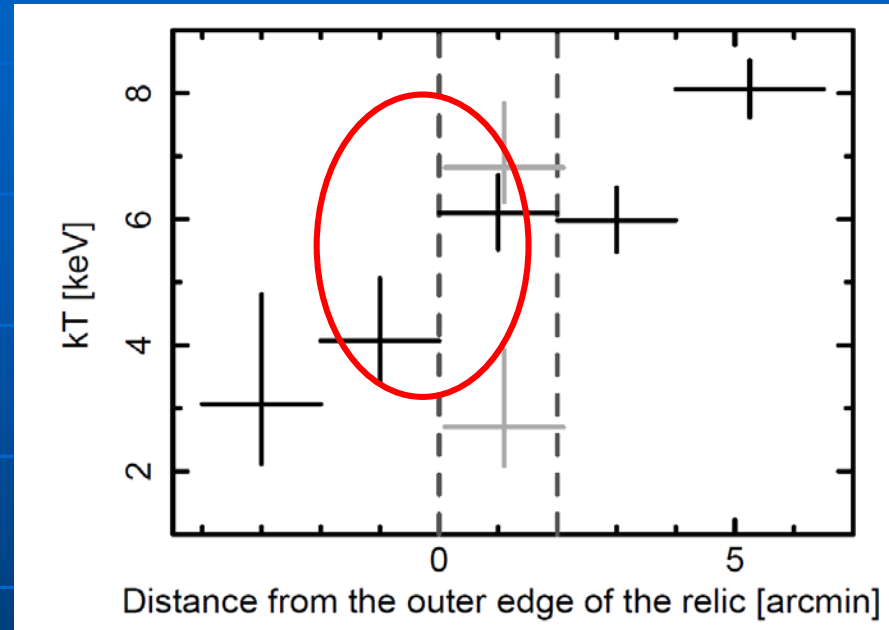
---->

$$M_{radio} = 3.3 - 4.6$$

toothbrush-relic: temperature profile across the relic (Itahana et al. 2015)



Colors: X-ray(Suzaku)
Contours: radio(WSRT)



- Obtained Mach number

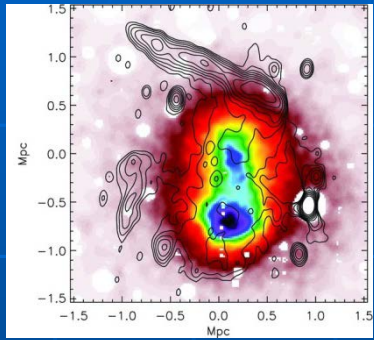
$$1.50^{+0.37+0.25+0.14}_{-0.27-0.24-0.15}$$

- Cf. updated radio results infer ~ 3

$$\frac{T_2}{T_1} = \frac{5M_X^4 + 14M_X^2 - 3}{16M_X^2}$$

Comparison with XMM results

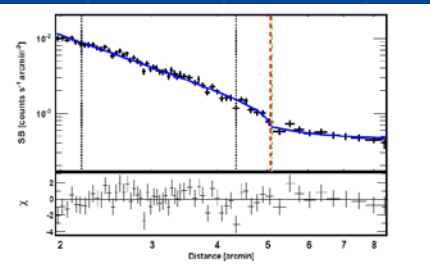
- Ogorean et al. (2013) obtained a similar Mach number for the toothbrush relic with XMM data.



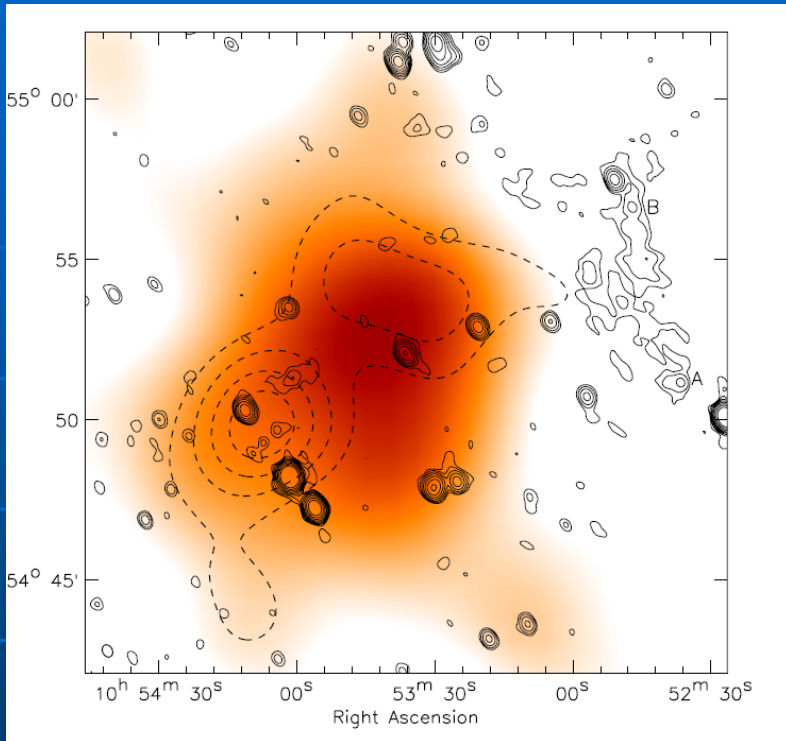
- Their results are based on X-ray surface brightness distribution analysis, which is much more severely affected by line-of-sight projection effects and, in principle, some assumptions are necessary for 3D density distribution.

$$\frac{\rho_2}{\rho_1} = \frac{4M_X^2}{M_X^2 + 3}$$

- Our results are more robust and model-independent.



RXC J1053.7+5453



van Weeren (2011)

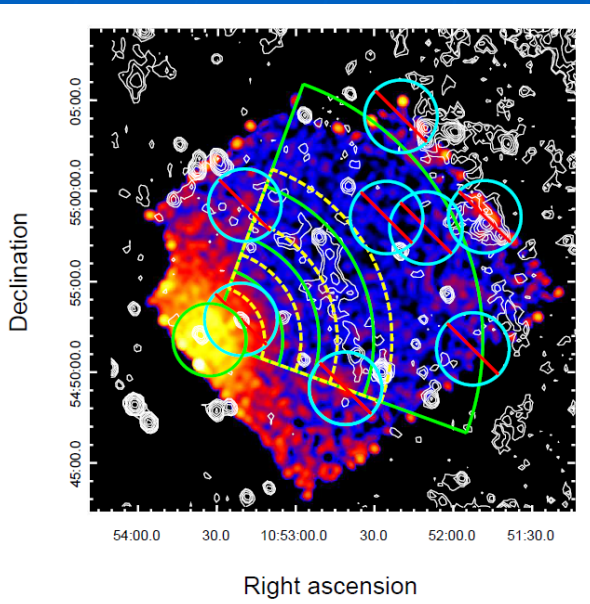
Colors: X-ray(ROSAT)

Solid contours: radio(WSRT)

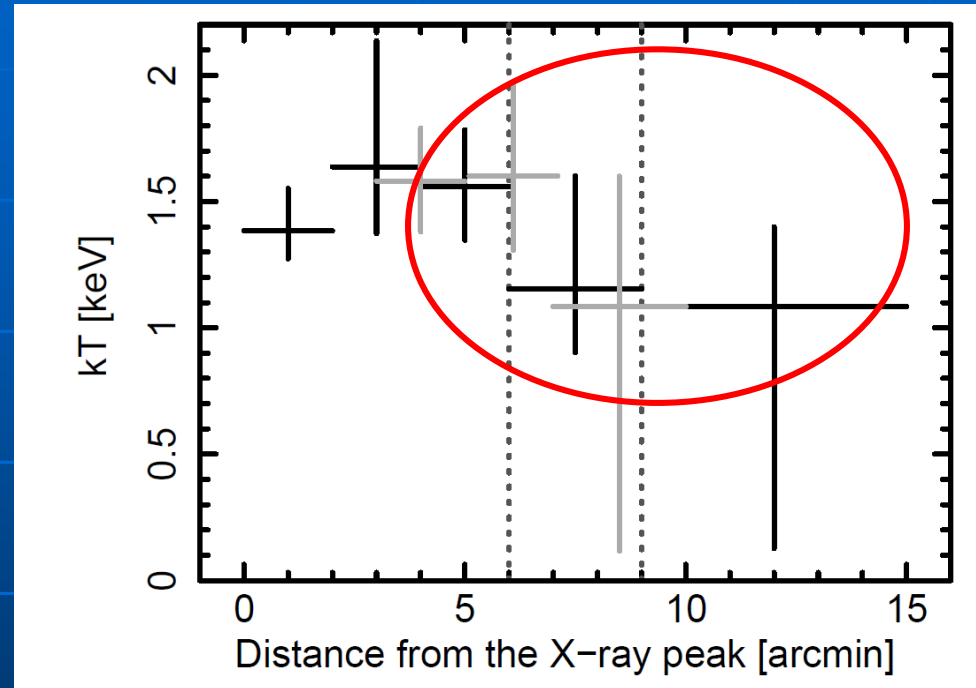
Dotted contours: galaxy distribution

- Elongated X-ray morphology, with radio relic (van Weeren et al. 2011)
- Two subgroups in galaxy distribution.
- No direct temperature measurements ($kT \sim 3\text{keV}$ is expected from L_x - kT relation)
- No radio spectrum information

RXC J1053: temperature profile across the relic (Itahana et al. 2017)



Colors: X-ray(Suzaku)
contours: radio(WSRT)

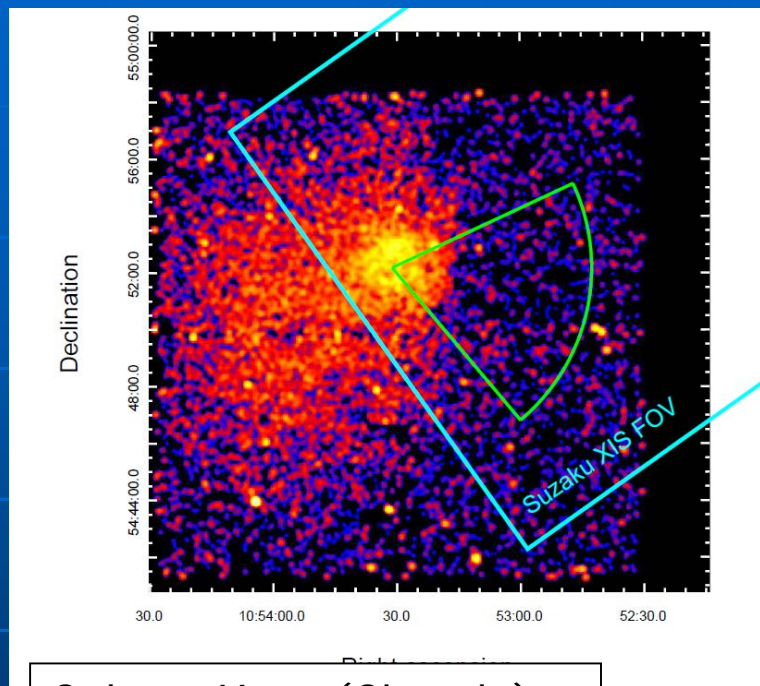


$$\frac{T_2}{T_1} = \frac{5M_X^4 + 14M_X^2 - 3}{16M_X^2}$$

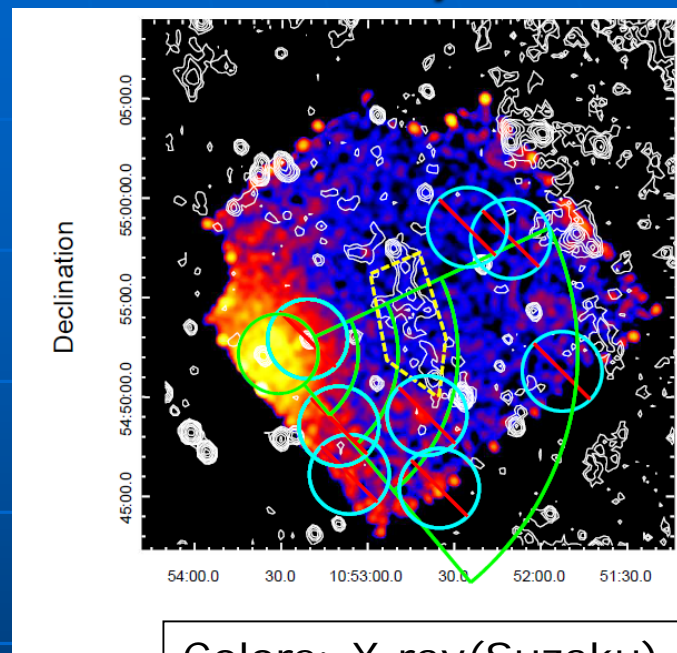
$$M_X = 1.44^{+0.48+0.14+0.03}_{-0.91-1.34-0.04}$$

- Unfortunately, we do not have any radio spectral information.

RXC J1053: Surface brightness edge (Itahana et al. 2017)



Colors: X-ray(Chanda)



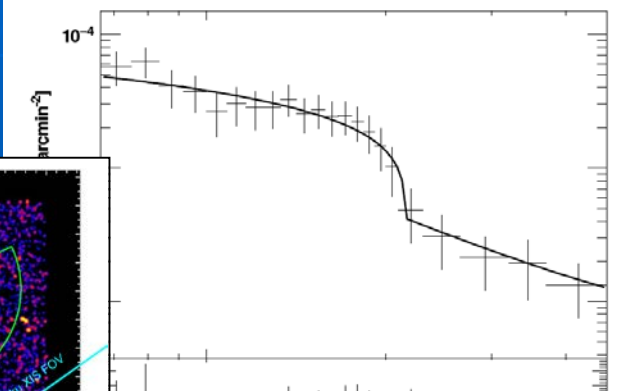
Colors: X-ray(Suzaku)
contours: radio(WSRT)

- We found surface brightness edge, between the cluster X-ray peak and relic.
- This indicates the discontinuity in density structure.
- Shock?, contact discontinuity?, others?

RXC J1053: Surface brightness edge (2)

(Itahana et al. 2017)

Surface brightness profile



$$n(r) = \begin{cases} n_1 \left(\frac{r}{R_f}\right)^{-\alpha_1}, & r < R_f \\ n_1 \frac{1}{C} \left(\frac{r}{R_f}\right)^{-\alpha_2}, & r > R_f \end{cases}$$

Temperature profile

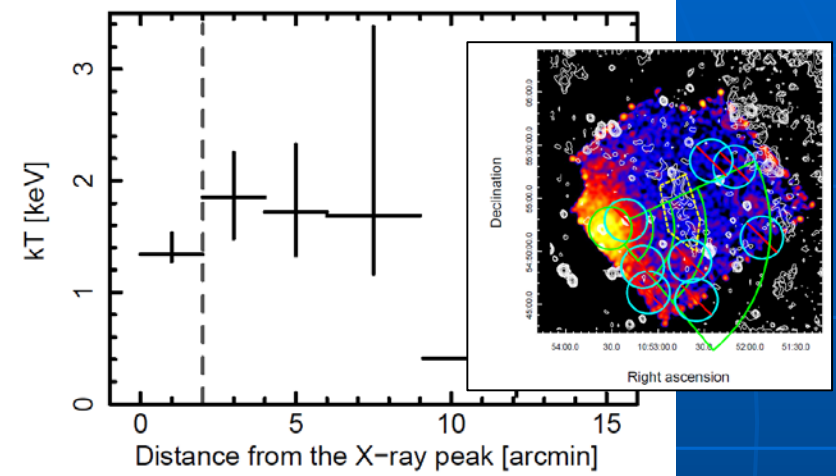


Fig. 8. The temperature profile across the surface brightness edge. The position of the surface brightness edge is displayed by dark gray dotted line.

$$n_1/n_2 = 2.44^{+2.50}_{-1.22}$$

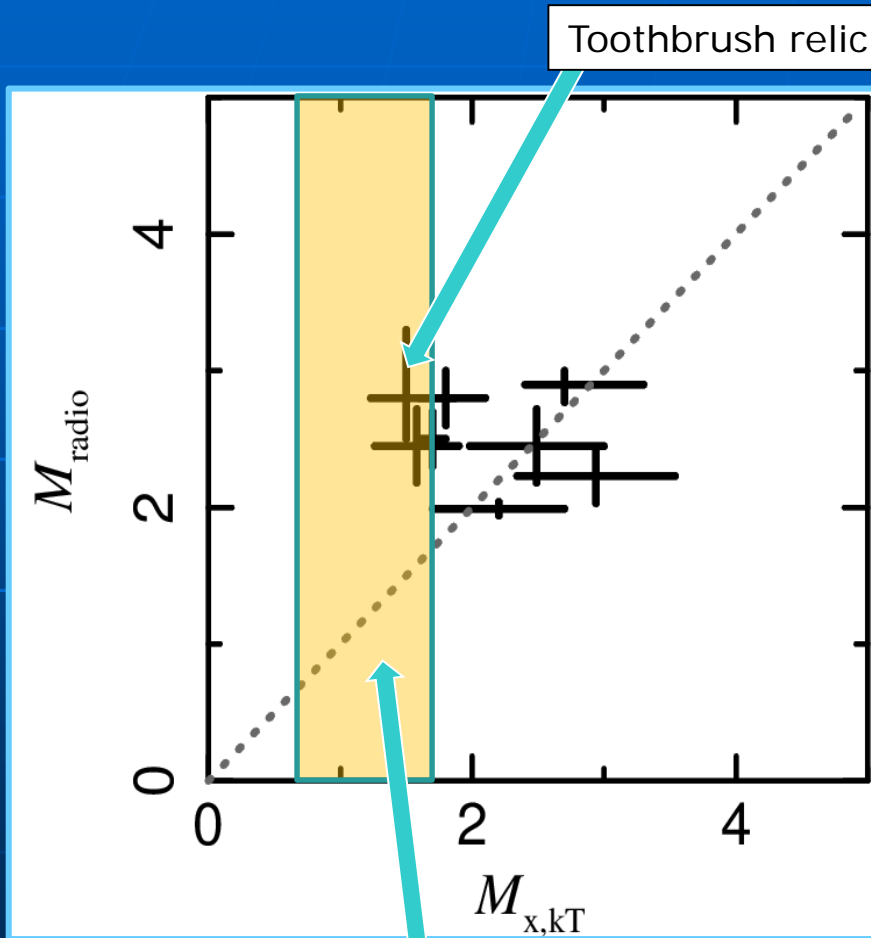
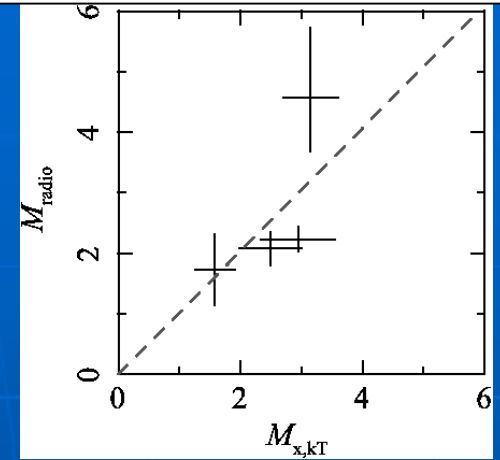
$$T_1/T_2 = 0.72^{+0.24}_{-0.15}$$

$$P_1/P_2 = 1.76^{+1.89}_{-0.95}$$

- This is not a shock, may be a contact discontinuity.

Radio relic Mach number problem: updated version

Akamatsu&Kawahara (2013)



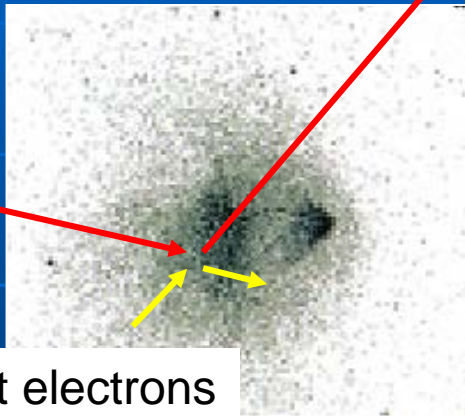
Region for RXC J1053

- Sample size becomes slightly larger.
- Some radio results has been changed.
- Basically, M_x and M_{radio} seems to be consistent with each other, but some outliers like "toothbrush" may exist.

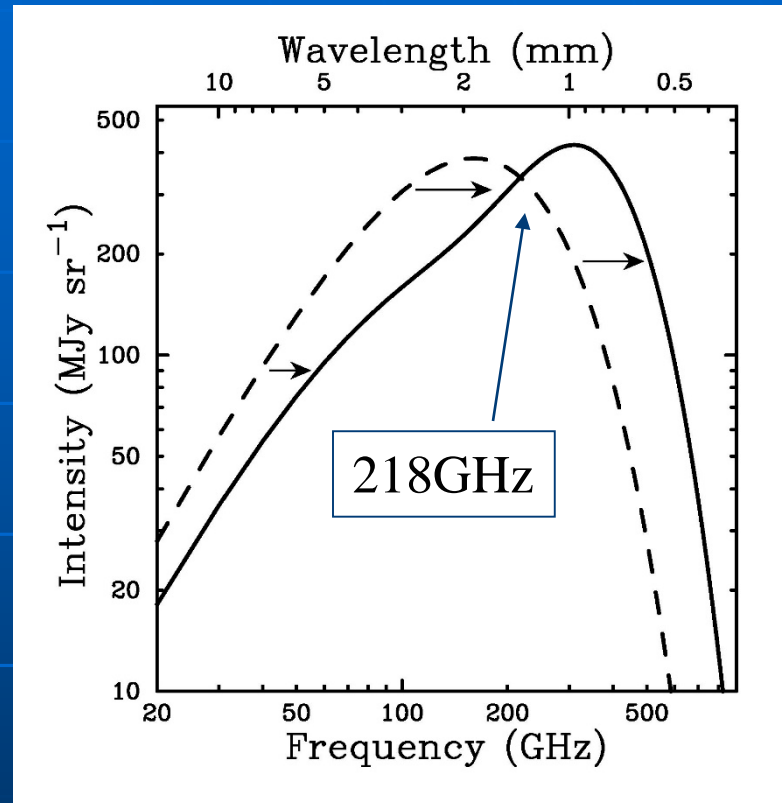
Sunyaev-Zel'dovich effect

Inverse Compton Scatterings

CMB photons
(2.7K black body)



Hot electrons
($10^{7-8}K$)



Cosmic Microwave Background (CMB) spectrum is modified because of inverse Compton scattering with hot gas such as ICM

- Decrement in mm band (R-J side)
- Increment in sub-mm band (Wein side)

SZ vs X-ray

$$I_X \propto \int n_e^2 T_e^{-1/2} dl$$

$$I_{SZ} \propto \int n_e T_e dl$$

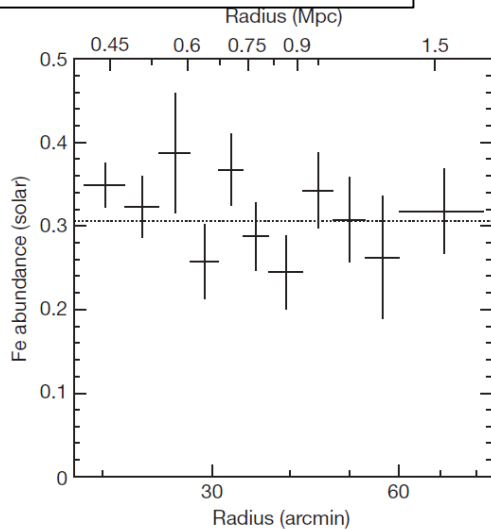
X-ray is more sensitive to density structures, while SZ is relatively sensitive to temperature structures.

$$I_X \propto (1+z)^{-4}$$

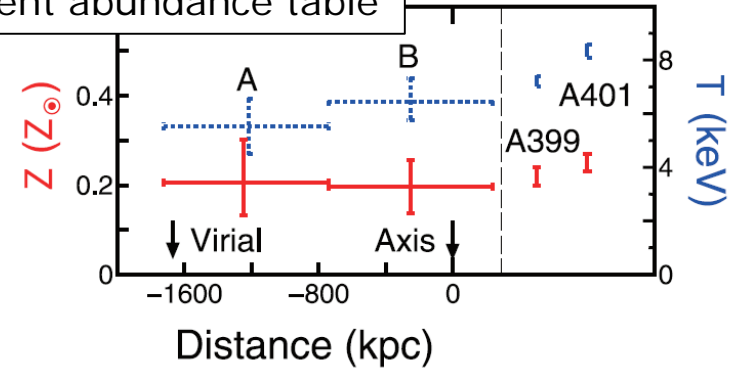
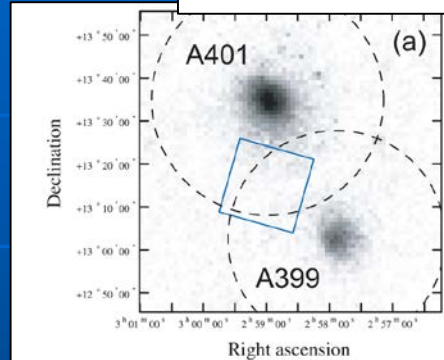
$$I_{SZ} \propto (1+z)^0, \text{ because } U_{\text{CMB}} \propto (1+z)^4$$

Metal Abundance in the outskirts of galaxy clusters

Fe abundance of Perseus cluster
Werner et al. (2013)

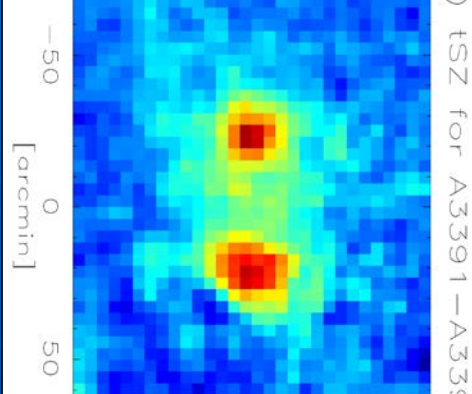


A399&A401
Fujita et al. (2008)
 $Z \sim 0.3$ with recent abundance table



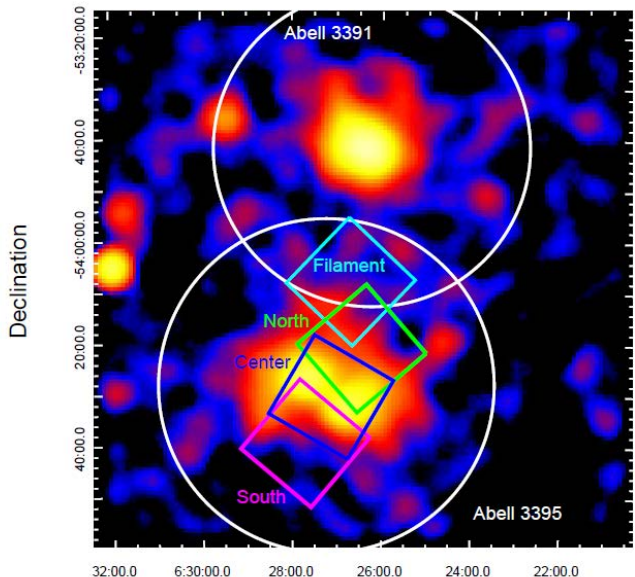
- Metal abundance in the cluster outskirts contains crucial information about transport processes of heavy elements from galaxies to the intergalactic space.
- There are only a few limited examples of the abundance measurements at the virial radius of clusters (A401&A399, Perseus, Virgo), because they are faint.
- $Z \sim 0.3$ solar, relatively high, which suggest an early enrichment scenario owing to outflows powered by SNe and/or AGNs.
- We need more samples.

SZ effect intensity map
Planck Collaboration(2013)



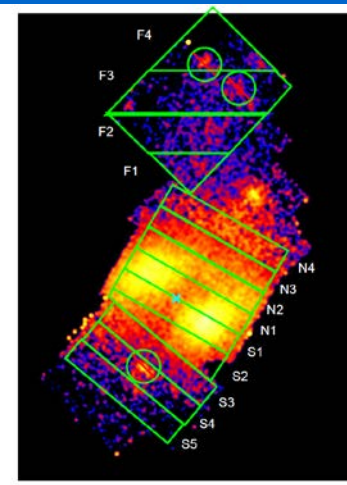
Abell 3395 & Abell 3391

- Virial radii are overlapped with each other. pre-merger?
- Hot ICM in the linked region
 - Diffuse X-ray emissions are detected with ROSAT and ASCA (Tittley & Henriksen 2001).
 - SZ effect detection (Planck Collaboration 2013)
- Because of the interaction of two clusters, the linked region is relatively bright, and suitable for the measurements of the abundance (similar to A399&A401).

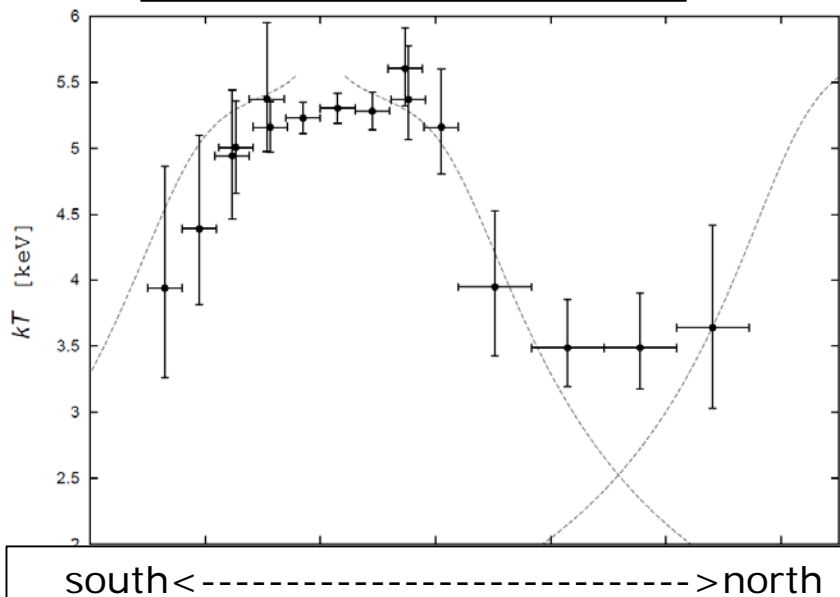


A3395&3391
ROSAT image
White circles: virial radii
Squares: Suzaku XIS FOV

A3395&3391: kT distribution (Sugawara et al. 2017)

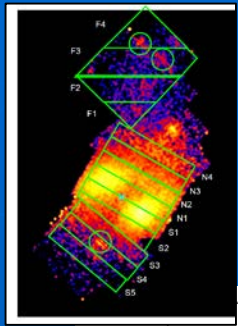


kT distribution
Dotted line: universal kT
profile proposed by
Okabe et al.(2014)

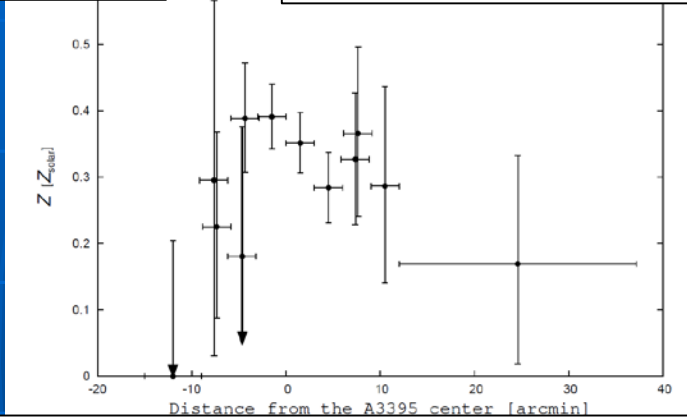


- kT distribution from the north of A3395 to the south (region connecting to A3391)
- The results are compared with the universal kT profile proposed by Okabe et al.(2014)
- Linked region have relatively high kT
----->
A hint of ICM heating because of merger??

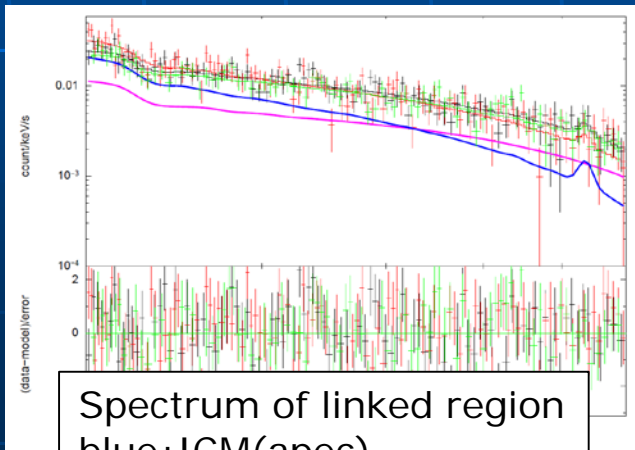
A3395&3391: abundance distribution (Sugawara et al. 2017)



Abundance distribution



south <-----> north



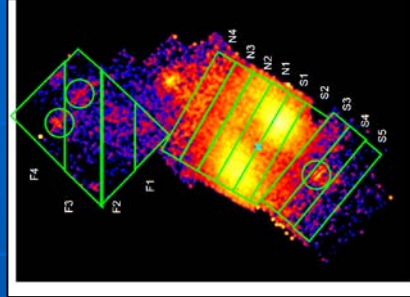
Spectrum of linked region
blue: ICM(apec)
magenta: CXB

- Spectral fit in the energy range of 2-7 keV (to remove impacts of Fe-L lines)
- In the linked region, we get $Z = 0.169^{+0.164+0.009+0.018}_{-0.150-0.004-0.015}$ solar.
- Consistent with the former results such as A399&A401, Perseus ($Z \sim 0.3$).
- Suggest the early enrichment scenario
- If we fit in the range of 0.7-7 keV, $Z < 0.120$ (Fe-L bias, Sasaki et al. 2015, Simionescu et al. 2015)

A3395&3391: Comparison with SZ results (Sugawara et al. 2017)

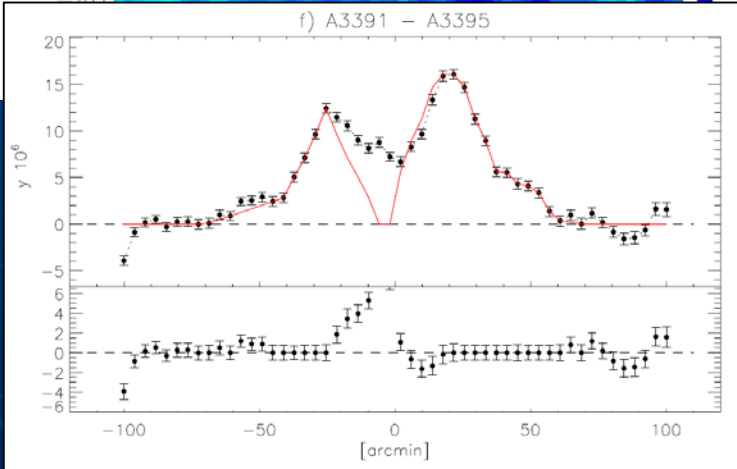
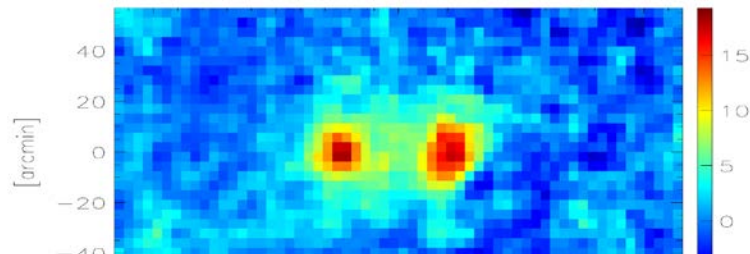
y-parameters in the linked region derived from the X-ray results

Region Number	$y (10^{-6})^*$
F1	$4.28^{+0.67+0.54+0.12}_{-0.60-0.68-0.13}$
F2	$2.90^{+0.31+0.41+0.13}_{-0.25-0.37-0.12}$
F3	$2.74^{+0.33+0.39+0.15}_{-0.25-0.36-0.13}$
F4	$2.95^{+0.64+0.54+0.19}_{-0.51-0.58-0.22}$



$$y = \int \left(\frac{kT_e}{m_e c^2} \right) n_e \sigma_T dl,$$

Planck Collaboration (2013)



- Assuming a simple geometry like cylinder, we obtained Compton y parameters only from the X-ray results (kT , n_e). $\rightarrow \sim 3 \times 10^{-6}$
- Our results are clearly smaller than the Planck results ($\sim 7 \times 10^{-6}$).
- Elongated structures along the line-of-sight? (or inclined cylinder?)
- kT might be underestimated?

About discrepancy of y parameters (geometrical factor etc)

- Assuming line-of-sight length L , normalization of apec model (ICM X-ray emission) is $N \propto n_e^2 L$
- Compton y parameter is $y \propto n_e L$
- Therefore, with fixed N , $y \sim L^{1/2}$
- If the assumed L is smaller than the actual L , y parameter will be underestimated.
- If the discrepancy is only owing to this geometrical effect, line-of-sight length should be ~ 5 times longer than the assumed value.
- A similar situation is realized if the filament is inclined to the line-of-sight direction only by ~ 10 degree.
- The difference seems too large to be explained by the geometrical effect.
- Other causes may be necessary (underestimation of X-ray kT measurements??).

Summary

- Diffuse non-thermal radio emissions are found in some clusters of galaxies (radio halos, relics).
- Radio relics are likely associated with shocks in the ICM.
- Comparison with X-ray and radio observation results provide us with implications of diffusive shock acceleration model.
- SZ and X-ray observations give complementary information of ICM.
- In A3391 and 3395 filament, apparently inconsistent results are obtained from X-ray and SZ results, which give us information about geometrical structures and possible hidden heated gas.